Geospatial Terrain Analysis of Sediment Sources within the Arroyo Mocho Watershed

by Paul Bigelow[1], Sarah Pearce[2], Lee Benda[3], Kevin Andras[3], Lester McKee[2], and Jamie Kass[2]
[1]Bigelow Watershed Geomorphology, [2]San Francisco Estuary Institute, [3]Earth Systems Institute

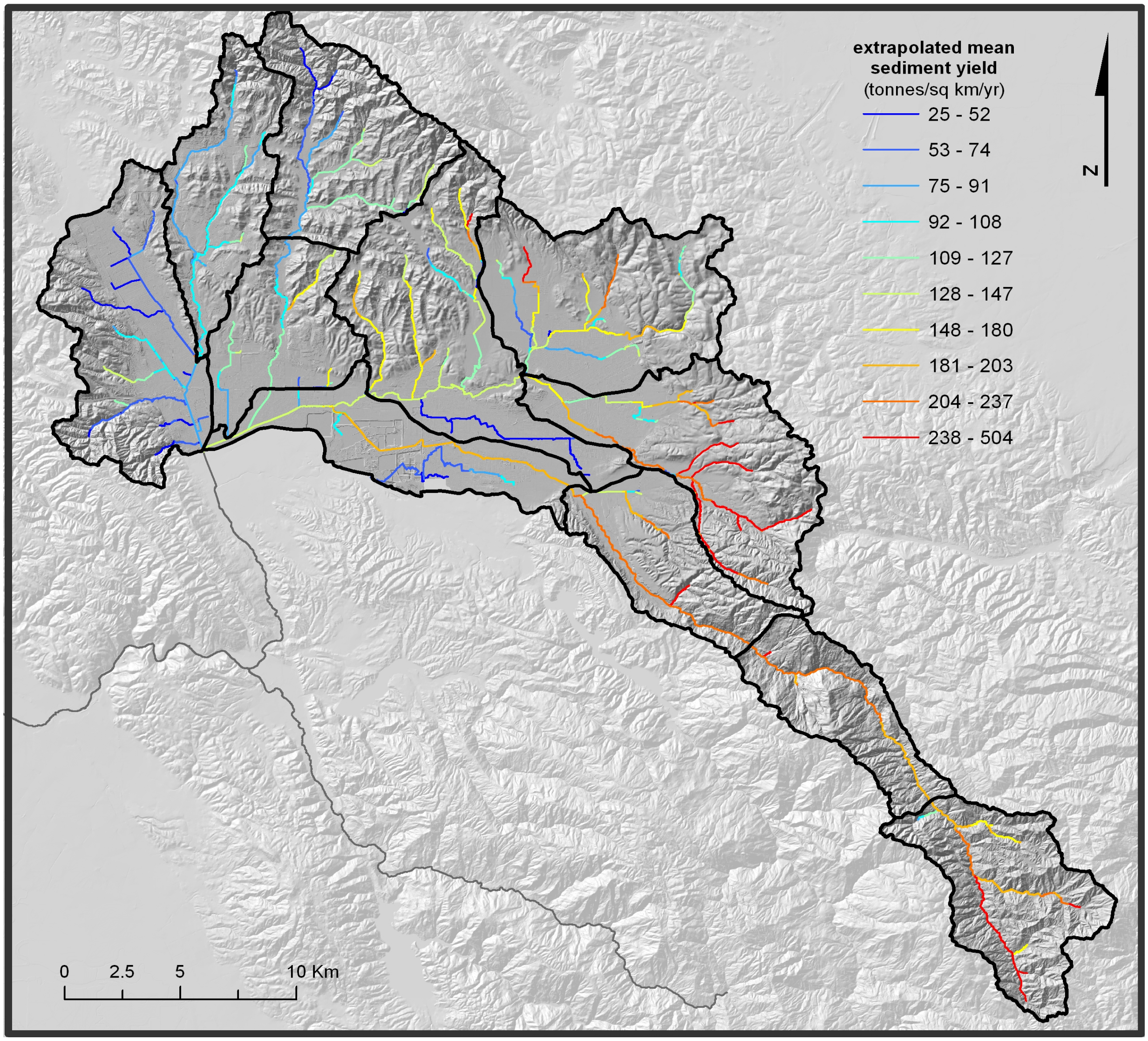

prepared for the Zone 7 Water Agency, Livermore, CA
May 2012 Draft for Review

bigelow watershed geomorphology

Earth Systems Institute

Suggested citation:

Bigelow, P., S. Pearce, L. Benda, K. Andras, L. McKee, and J. Kass. 2012. Geospatial Terrain Analysis of Sediment Sources within the Arroyo Mocho Watershed. Prepared for Zone 7 Water Agency, Livermore, CA.

Introduction and Objective

Zone 7 Water Agency provides drinking water and flood protection for the greater Livermore Valley. The District maintains ~ 59 km (37 miles) of flood control channels that transport water runofff and sediment from the Arroyo Mocho watershed (Figure 1). The sedimentation that occurs in some of the channel facilities is associated with a combination of erosion and sediment supply, channel geometry, basin hydrology and channel vegetation. In order to maintain channel flood capacity, the city of Livermore has conducted periodic channel de-silting of aggraded areas near bridges. Zone 7 has contracted with the SFEI team to better understand channel depositional processes to potentially defray costs and regulatory burden for de-silting aggraded areas. With improved understanding of erosion and sediment sources, there may be opportunities to reduce channel sedimentation. Opportunities may include adjustments to channel geometry, characterizing upstream erosion with the goal of identifying controllable sources, and analyzing historic conditions to identify areas that are prone to sedimentation. Improved understanding may lead to innovative management strategies that can include upstream mitigation of erosion sources. As part of these goals, *the objective of the terrain mapping sub-task is to characterize the spatial distribution of sediment sources throughout the watershed*.

Background

Arroyo Mocho drains the Livermore Valley westward towards the San Francisco Bay via Arroyo de la Laguna and Alameda Creek. Upstream of the confluence with Alamo Creek (where it becomes Arroyo de la Laguna), Arroyo Mocho watershed drains an area of 573 km^2 and contains the tributary watersheds of: Alamo Creek (Canal), Chabot Canal, Tassajara Creek, Line G-3, Cottonwood Creek, Collier Canyon Creek, Cayetano Creek, Arroyo Las Positas, Altamont Creek, Arroyo Seco and upper Arroyo Mocho (Figure 1). The estimated stream network length within the Arroyo Mocho watershed is 193 km (SFEI 2011). Elevation ranges between 60 and 1230 m (Figure 1) and mean annual precipitation averages 428 mm (17 in) in Pleasanton (Figure 2, Prism 2012). Land use includes urban and commercial in the valley and lower slopes, agricultural (primarily grazing and viticulture), and forested and non-forested lands in the upper watershed.

The watershed is underlain by a sequence of folded and faulted Miocene sedimentary units, Plio/Pleistocene Livermore Gravels, Quaternary valley fill alluvium, and Cretaceous Franciscan Formation (Graymer et al. 1996, Helley and Graymer 1997). Landslide mapping shows a number of large, deep-seated landslides in the upper Arroyo Mocho canyon, and many shallower, earthflow type landslides in the northern tributaries (Davenport 1985, Wentworth et al. 1997, Roberts et al. 1999, Majmundar 1991 and 1996).

The southern portion of the Arroyo Mocho sub-watershed is characterized by steep topography and rugged hillslopes that have experienced large mass movements (landslides) in the geologic past. Currently the channel flows through a steep, narrow canyon in the lower portion of the sub-watershed. Although the hillslopes remain steep in the upper portion of the sub-watershed, the stream gradient decreases, creating a gentler, slightly wider valleys. The eastern portion of the watershed, primarily the Arroyo Seco and Altamont Creek sub-watersheds, are of

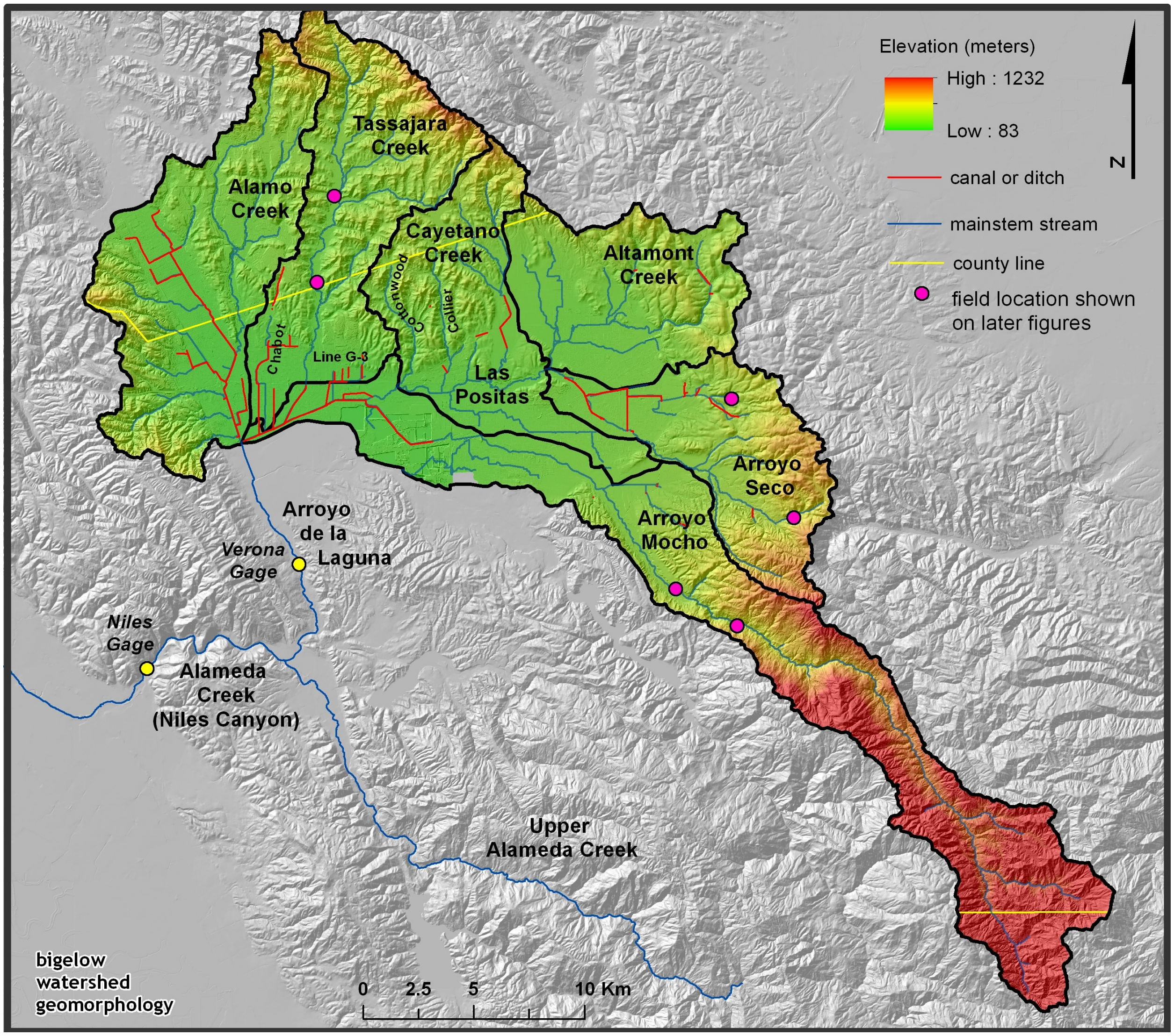

Figure 1. Arroyo Mocho watershed showing the six major basins, mainstem channels, and flood control channels.

lower elevation, less steep rolling grassy hills that grade into the eastern portions of the valley floor. The northern sub-watersheds (Alamo Canal, Chabot Canal, Tassajara Creek, Line G-3, Cottonwood Creek, Collier Canyon Creek, and Cayetano Creek) have lower portions that are gentle rolling grassy hills that grade into wide valley floor surfaces. The upper portions contain steeper topography reflecting the underlying bedrock geology.

Historically the watershed contained many creeks that flowed from the canyons and spread across the valley floor, depositing their sediment and recharging groundwater. These distributary channels built broad alluvial fans that graded into the wide valley floor surface. At the western edge of the valley was the Pleasanton lagoon (Tulare Lake), a wetland that trapped sediment and recharged ground water. However, following over 100 years of land use,

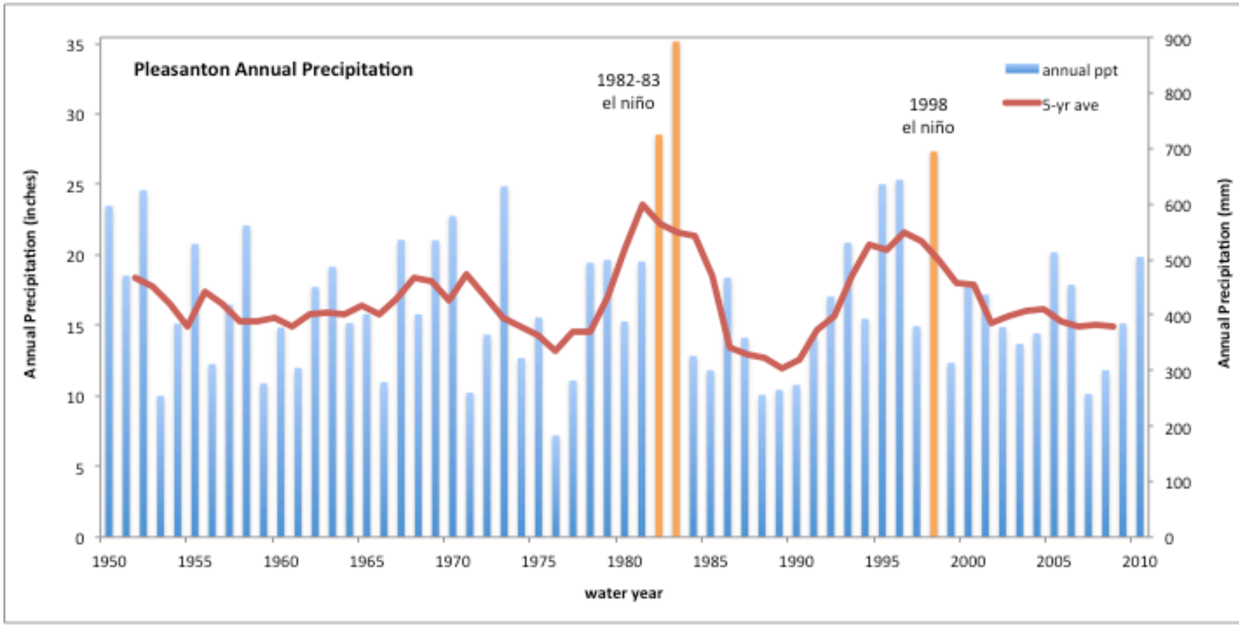

Figure 2. Mean annual precipitation over the past 60 years for Pleasanton, California (Prism 2012).

including urban development and associated channel modifications, the channels now have direct connections from the upper watersheds, across the valley floor, to the outlet of Arroyo de la Laguna (via artificial channels in most locales). These changes have fundamentally altered the Livermore Valley floor from a sediment sink to a sediment conduit with increases sedimentation potential downstream.

Currently a variety of erosional processes are observed, including hillslope mass movement, soil creep, gullying, channel bank erosion and bed incision, and land-use related erosion (e.g. roads, grazing, construction). However, the location and relative magnitude of these processes are known to vary in relation to underlying geology, soils, aspect, slope and convergence, vegetation, and landuse/land management. Therefore we anticipate that the dominant processes and resulting sediment supply will vary considerably from one sub-watershed to another in the area of Zone 7 interest.

Methods

We generated a digital terrain model using NetMap, a watershed analysis tool that provides spatially registered and largely automated mapping of watershed features that govern erosion, network, valley and channel morphologic types, and sources of riverine habitat heterogeneity. NetMap is tailored for a variety watershed and geomorphic analyses across the Pacific Northwest, Pacific Rim, and parts of Europe (see netmaptools.org Benda et al. 2007, 2009, 2011). The primary steps in the terrain mapping included:

1. Development of an attributed stream layer and erosion potential grid[1] using NetMap in conjunction with a high resolution DEM.

2. Generatation of a vegetation height grid to modify erosion predictions.

3. Prediction of relative erosion potential throughout the study basin (focused along stream channels) using the vegetation and erosion grids.

4. Conversion of the erosion potential to sediment yield based on gage data.

5. Aggregation of the erosion predictions at various scales: reach, subwatershed, basin.

6. Field validation of erosion predictions in the field.

DEM and Stream Network

An attributed stream channel network was delineated using a 2m DEM based on algorithms for flow direction and channel delineation described by Clarke et al. (2008). The DEM was compiled and resampled from a 0.3 m DEM for Alameda County and a 3 m DEM for Contra Costa and Santa Clara Counties, both derived from Light Detection and Ranging (LiDAR)[2] data collected by the USGS. The channel network was divided into a linked set of channel segments (ranging from 2 – 80 m length, ave 30 m). Contributing area and channel length were calculated from the DEM for each segment. Bankfull channel width and depth and mean annual flow were estimated using available regional regressions:

$$\text{bankfull channel width (m)} = 3.3494\ (\text{drainage area [km}^2])^{0.3737} \qquad (1)$$

$$\text{bankfull depth (m)} = 0.3593\ (\text{drainage area [km}^2])^{0.3593} \qquad (2)$$

Bankfull channel width and depth regressions were derived for the “San Francisco Bay Area” with no data points or correlation coefficient provided (Dunne and Leopold 1978), but the streams used to derive the curves “were from near Leopold’s residence in Berkeley (a listing of sites was not separately maintained)” (Emmet 2004). Each segment of the channel network was attributed with suite of parameters calculated from the DEM including elevation, drainage area, stream gradient, stream order (Strahler 1957), valley width, debris flow probabilities (scour, passage, deposition, tributary confluence effects probabilities, and intrinsic potential for salmonid habitat by species, and many more attributes (see Miller 2003 and Benda et al. 2007 for details). From these attributes, others can be calculated for example, stream power

---

[1] A GIS grid defines geographic space as an array of equally sized square grid points arranged in rows and columns. Each grid point stores a numeric value that represents a geographic attribute (such as elevation or surface slope) for that unit of space. Each grid cell is referenced by its x,y coordinate location (http://en.wikipedia.org/wiki/Esri_grid)

[2] LiDAR is an optical remote sensing technology that measures the distance to a target (surfaces) with light, often using laser pulses from an aircraft. Because LiDAR penetrates through vegetation canopy to the land surface and can be collected at high spatial densities, it can be used to develop high resolution DEMs to detect subtle topographic features such as landslide terrain, river terraces, and river channel banks.

(drainage area * gradient), valley width index (valley width/channel width), etc. All of the NetMap data layers generated for Zone 7 are available at netmaptools.org/coverage and the analyses tools at netmaptools.org/analysis_tools.

Generic Erosion Potential (GEP)

Erosion in the form of shallow landslides, gullies and surface erosion is often driven by slope steepness and slope curvature (Dietrich and Dunne 1978, Sidle 1987). To estimate a measure of erosion potential in the watersheds, a dimensionless index in NetMap that employs slope gradient and local topographic convergence was used (Miller and Burnett 2007a, Benda et al. 2011):

$$GEP = (AL \cdot S)/b \qquad (3)$$

where GEP is the generic erosion potential, b is a measure of local topographic convergence (the length of an elevation contour crossed by flow out of a pixel, values less than one pixel indicate convergent topography), AL is a measure of local contributing area (within one pixel length) and S is slope gradient (Miller and Burnett 2007a). GEP is a dimensionless index of erosion potential with values from 0 – 1, where larger values correspond to steeper, more convergent topography. Steeper, more convergent topography (e.g., higher values of GEP) should correspond to higher landslide densities and, in areas prone to surface erosion, to higher gully-initiation-point densities. Thus, GEP is a relative measure of erosion potential that encompasses processes of shallow landsliding, gullying, and surface erosion that is applicable to both humid and semiarid landscapes.

Limiting Estimates to Near Stream Sources

During field work and based on satellite imagery (Google Earth) we observed that many of the channels had an arroyo form: an incised topography within a broad valley floor, with steep and occasionally bare eroding banks. These raw banks appear to dominate the chronic (annual) supply of sediment to channels in the study basin (and thus the main source of sediment to the aggrading channels downstream in flood control areas). Often at the top of the arroyo bank, a flat valley floor exists, with essentially no sediment production or delivery to the channel. In addition, in the steeper channel reaches most of the sediment production occurred on the channel banks and hillslope areas adjacent to the channel; hillslopes farther removed from the channel did not appear to be delivering sediment on an annual basis. Based on these observations, we confined the analysis of erosion sources to areas adjacent to channels (e.g., the arroyo landform). We chose a zone or buffer of 6x the bankfull width (equation 2) around the channel that generally captures the steep eroding banks of the arroyo channel form. The value of 6x was chosen based upon field observation and evaluation of test field locations, where values of 2x, 4x, and 6x were considered. The 6x buffer maximizes the inclusion of hillslope areas that appear to be contributing sediment annually, yet limits the area that is not contributing, for the majority of the channel network length. This approach excludes more episodic supply from mass wasting sources that are located further from the channel that require a long-term sediment budget approach to estimate (see later).

Effects of Vegetation on Erosion

During our initial field reconnaissance we observed that arroyo bank erosion was reduced by vegetation, where larger and denser vegetation created stable channel bottoms and banks. Reaches that had little to no vegetation tended to be more erosive compared to reaches that had shrubs or trees established on the banks. We hypothesize that the existing vegetation is reducing erosion by lessening raindrop impact, providing increased soil strength through the root network, reducing surface erosion, rill erosion, and shallow bank slumps and slips (e.g. Thorne 1990, Simon and Darby 1999, Abernethy and Rutherford 2001). This is true in particular in these arroyo channel systems because there is little organic groundcover in the absence of vegetation.

While bank erosion and landsliding can occur under vegetation, the fundamental role of vegetation in reducing erosion is well established (e.g. Thorne 1990, Simon and Darby 1999, Abernethy and Rutherford 2001). For example, the amount (percentage) of bare soil is related to surface erosion (Benavides-Solorio and MacDonald 2005) and bare soil should be inversely proportional to vegetation cover. In addition increasing tree age (and thus rooting extent and depth) is related to increasing stability of the soil (Sidle 1987). Consequently we developed a method that relates vegetation cover to our erosion potential index. We created an erosion reduction parameter based on vegetation height and density (2 m GIS grid) using the first (representing the tallest vegetation) and last (representing the ground surface) return LiDAR points. The GIS grid was truncated to heights between 0 – 42 m to remove artifacts common in raw LiDAR data and the resulting grid was processed with fill and inverse fill operations to remove local sinks and peaks. A tree height of 42 m was estimated to be maximum height for old growth deciduous or conifer trees in the watershed based on the known species of trees and their typical maximum heights. The last return raster was then subtracted from the first returns to produce vegetation height. The vegetation height grid was converted (normalized) to the same 0 – 1 scale as GEP based on our estimate of the relationship between tree height and bank stabilization (erosion reduction) (Figure 3):

$$\text{Erosion reduction} = 0.1906 \ln(\text{tree height in m}) + 0.136 \qquad (4)$$

Because the tree canopy height of each 2 m grid cell is represented, this grid also represents the density of vegetation, another factor that can reduce erosion (e.g. Beeson and Doyle 1995, Wang et al. 2004). Using equation 4, a grid cell with a tree canopy height of 1 , 21 , or 42 m would be normalized to 0-1 scale values of 0.14, 0.72, and 0.85, respectively (i.e. 14, 72, and 85% erosion reduction). Equation 4 was derived from (1) the general relationship between vegetation (tree) height and canopy width, rooting width and depth, and associated bank stabilization (e.g. Smith 1964, Tubbs 1977, Gilman 1988), and (2) our field observations of tree height and bank stabilization. Here, we generally observed that stability of the banks increases with vegetation height up to a maximum of 11 meters and then levels off. We generally observed that grasses were less effective than shrubs, and shrubs were less effective than larger trees in reducing arroyo bank erosion. The resulting erosion reduction grid was subtracted from the initial GEP grid to estimate erosion sources. For example, where a grid cell has a GEP value of 1 and a corresponding erosion reduction value of 0.5, the resulting modified

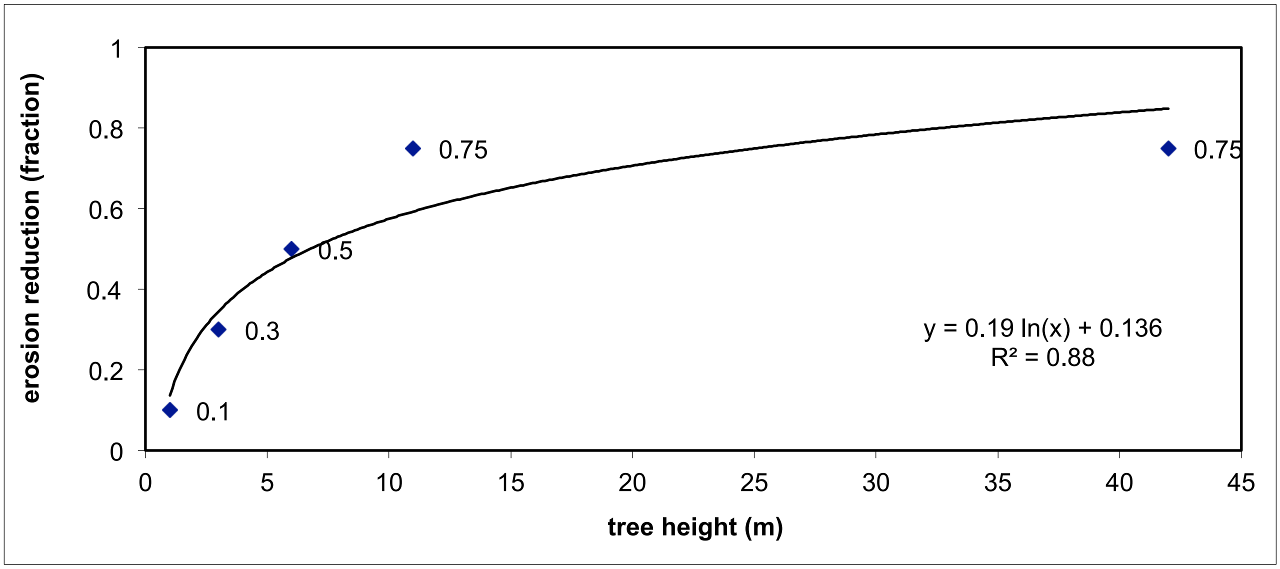

Figure 3. Estimated relationship between tree height and reduction in erosion (bank stabilization) used to reduce generic erosion potential (GEP) estimates (see text for details). Relationship based on field observations and the general relationship between vegetation and bank stability (see text for details).

GEP would be 0.5; where there was no vegetation, GEP values were unchanged. Maximum GEP reduction due to the greatest vegetation height was 0.85 (85%). We were unable to obtain raw LiDAR for Santa Clara County, so it was not possible to create a vegetation reduction grid for this small southeastern portion of the watershed at the headwaters of Arroyo Mocho canyon (Figure 1).

Conversion to Sediment Yield, Statistics, and Field Checking

Because GEP is a dimensionless index of erosion from 0 - 1, we converted GEP to sediment yield for a more useful and intuitive visual display of erosion across the watershed. To accomplish this in NetMap we linearly scaled the independently estimated sediment yield rate to GEP values. High values of GEP present higher erosion rates and lower values of GEP represents lower erosion rates. To obtain the conversion factor relating GEP to sediment yield in the study basin we used Equation 5:

$$conversion\ factor = Gep\ x\ \frac{mean\ sediment\ yield\ rate\ at\ Verona\ Gage}{mean\ GEP} \quad (5)$$

An average sediment yield rate of 155 tonnes km^{-2} yr^{-1} was used based on estimates from the Verona Gage on Arroyo De La Laguna (Figure 1) from 1994 – 2006 for the drainage area below reservoirs that includes both suspended and bed load (Bigelow et al. 2008). *The conversion of GEP to sediment yield value is an approximation but likely corresponds to the correct order of magnitude in the context of sediment budgeting technology (Reid and Dunne 1996).* Summary statistics were calculated for GEP and sediment yield at four scales: pixel (2m^2), reach (mean 586 m^2), subwatershed (mean 2.7 km^2), and tributary basin (mean 51 km^2). The erosion predictions were checked during two days of field observations and by draping erosion predictions over satellite imagery from Google Earth (i.e. converting erosion grids to .kml files).

Sediment Aggregation Downstream and Sediment Storage Potential
We also aggregated (summed and area weighted) the predicted sediment yield through the stream network to illustrate how sediment yield varies downstream through the channel network. The aggregated sediment yield value at the bottom of the watershed equals the basin average sediment yield. To identify areas prone to sediment storage that could be targeted for restoration (reconnection of channels to floodplains) we calculated the a sediment storage index for larger streams draining areas > 2 km^2:

$$storage\ potential = \frac{valley\ width\ index}{stream\ power\ index} \qquad (6)$$

where the stream power index is drainage area * gradient, and valley width index (e.g. Grant and Swanson 1995) is valley width (at 2x bankfull depth) /channel width (all of these parameters are available in NetMap). Stream power reflects the ability of a channel to transport or store sediment: streams with higher stream power have less opportunity to create large in-channel storage reservoirs in contrast with streams of lower power that can store sediment. The valley width index reflects the potential width of the flood plain for sediment storage.

Results

Erosion Predictions and Field Observations
GEP characterizes erosion in the form of shallow landslides, gullies and surface erosion that is driven by slope steepness and slope convergence. During a two-day field reconnaissance we observed steep eroding banks (bare of vegetation) in areas of high predicted GEP values, a result verified using Google Earth imagery (Figures 4 - 9). In addition, we observed much more stable banks in areas with lower GEP values. These observations indicate that the erosion predictions appear reasonable for delineating relative erosion potential within and between the watersheds in the Zone 7 study area.

Spatial Distribution of Sediment Sources
The spatial distribution of GEP and predicted sediment yield at the tributary basin scale (HUC 12 basins) varies considerably (Figure 10). At this largest scale, the more erosive areas are concentrated in the steeper dissected basins of the southeastern watershed, primarily the upper three Arroyo Mocho basins, Arroyo Seco, and Altamont Creek, where GEP values (and predicted sediment yield) are up three hundred percent higher than western areas at the basin scale (Figures 10). When the basins are grouped into entire tributaries, the Arroyo Mocho tributary dominates predicted sediment yield, supplying nearly half the total load (Figure 11). When viewed at the subwatershed scale (Figure 12), the more erosive subwatersheds (in red) are not isolated to a single larger basin, but generally are grouped in several steep or heavily incised areas across the entire Arroyo Mocho watershed, including steeper uplands

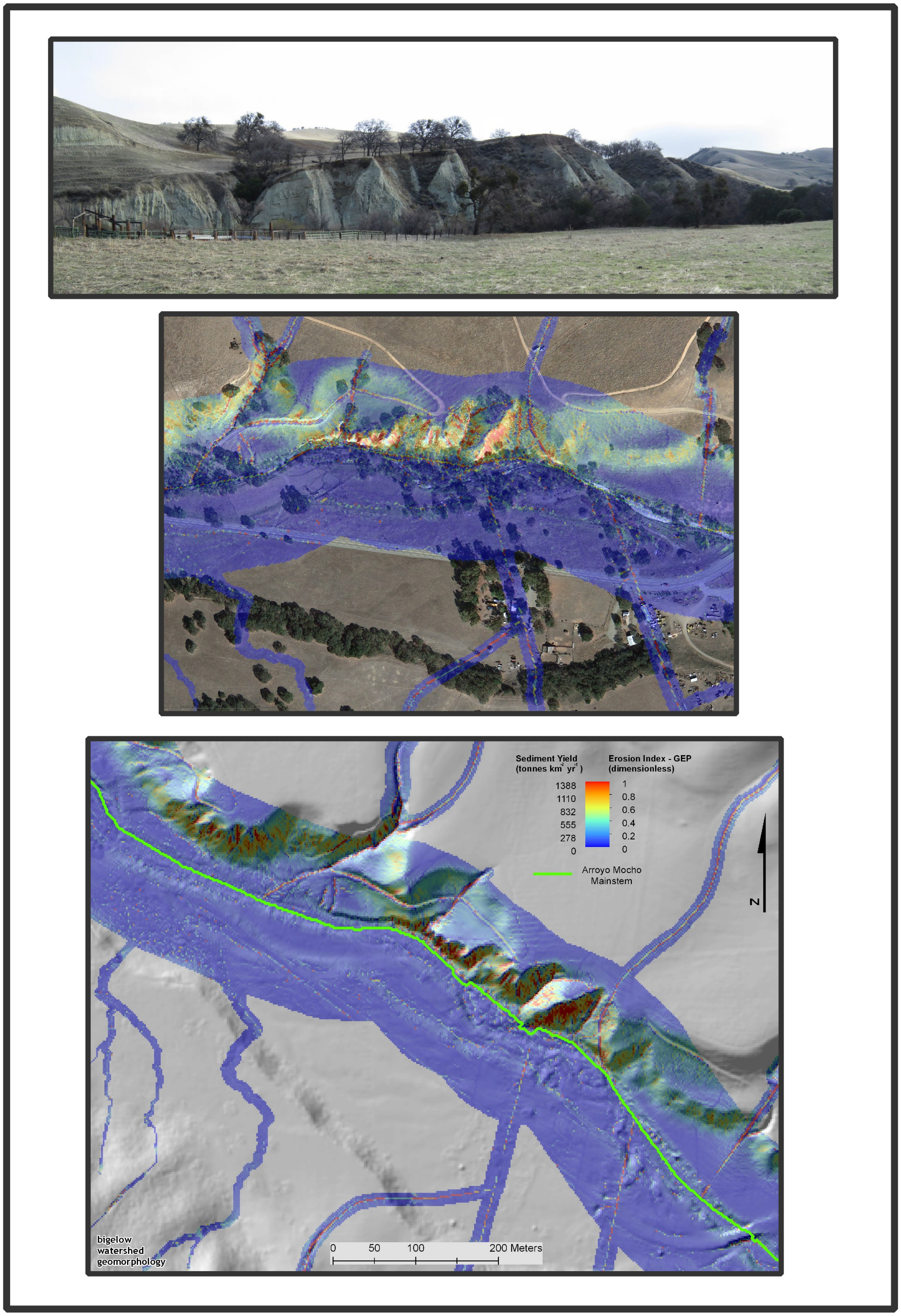

Figure 4. Eroding terrace in middle Arroyo Mocho basin, showing field photo (upper), and pixel scale modified GEP and predicted sediment yield values draped over Google Earth image (middle) and the 2m DEM (lower). Site location is shown on Figure 1. Initial GEP grid was derived from DEM using NetMap (Benda et al. 2007, 2011).

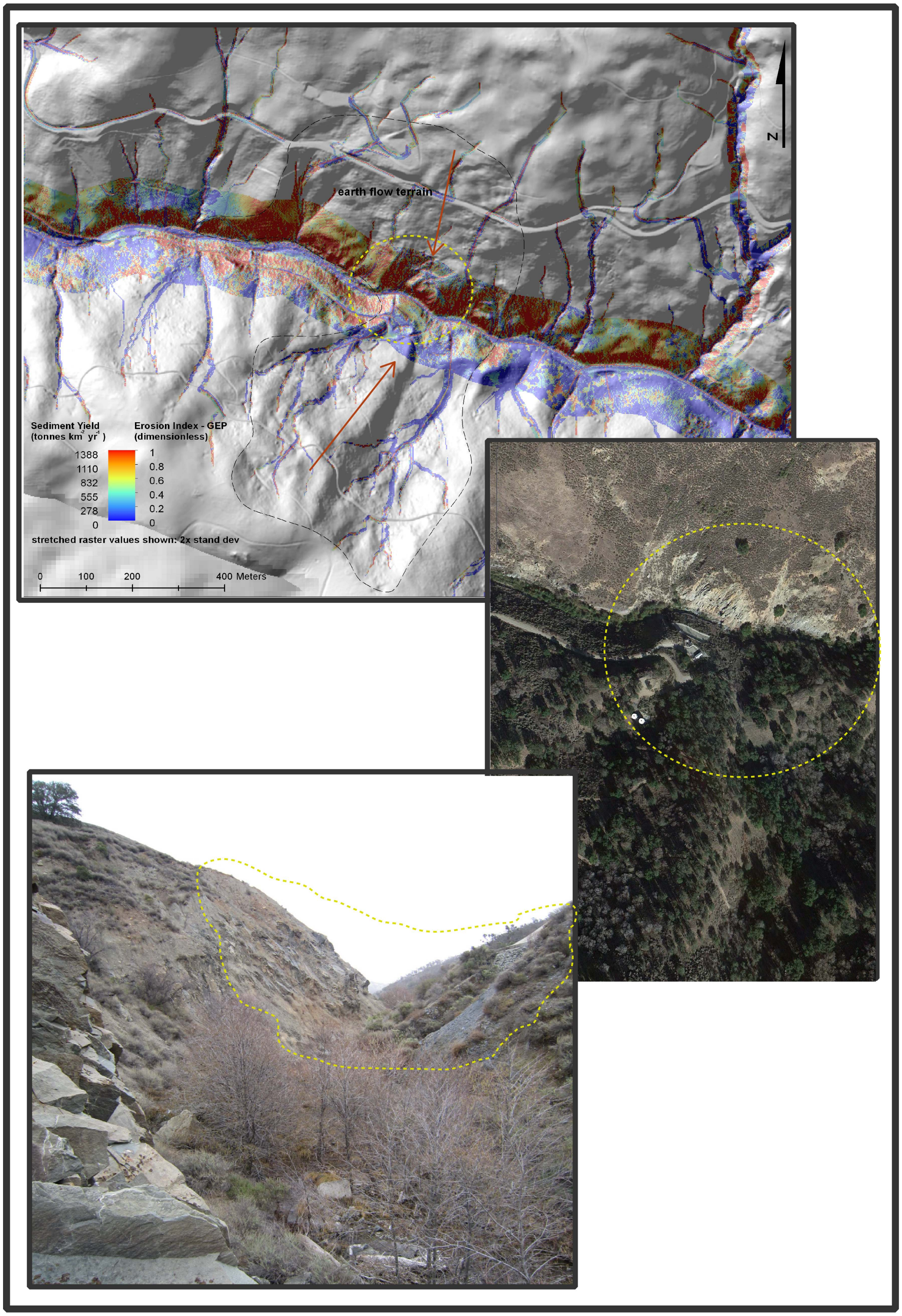

Figure 5. Deep-seated landslide/earthflow terrain in upper Arroyo Mocho basin, showing pixel scale modified GEP and predicted sediment yield values draped over the 2m DEM (upper), and Google Earth image (middle) and field photo (lower) showing the eroding earthflow toes. Site location is shown on Figure 1. Initial GEP grid derived from DEM using NetMap.

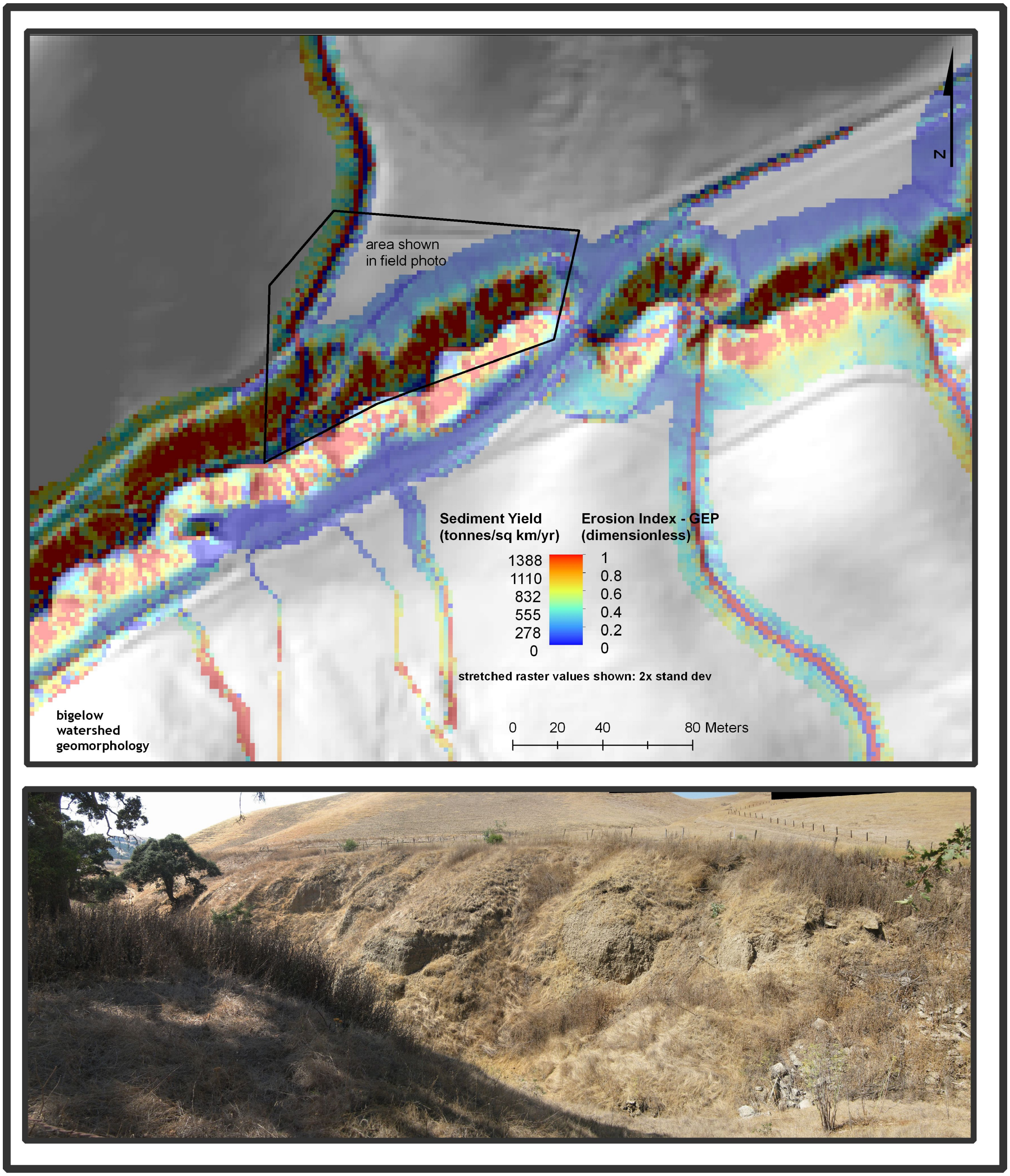

Figure 6. Incised channel and eroding bank in Arroyo Seco basin showing pixel scale adjuste GEP and predicted sediment yield draped over 2 m DEM (upper) and field photo (lower). Site location is shown on Figure 1. Initial GEP grid derived from DEM using NetMap.

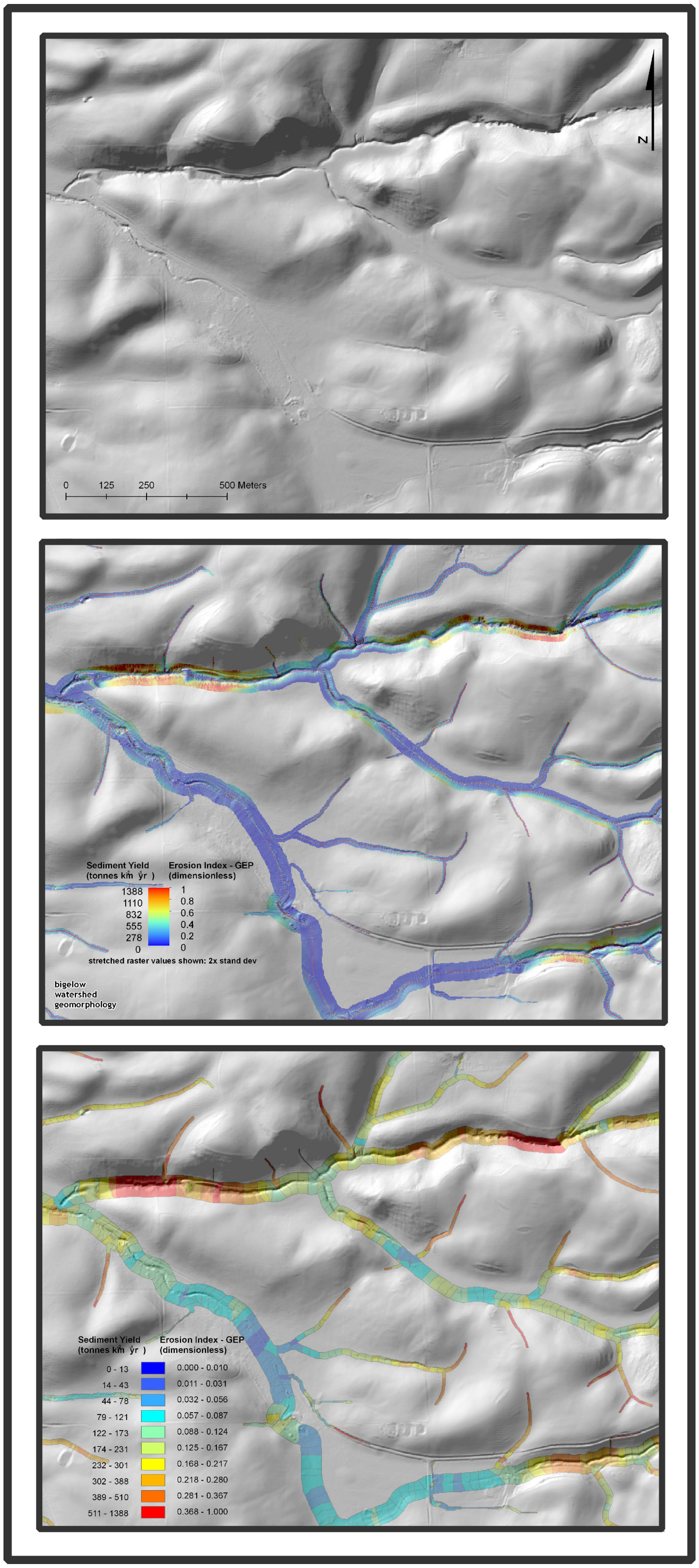

Figure 7. Patchy channel incision in Altamont Creek basin, showing channel incision on the 2 m DEM (upper) and pixel (middle) and reach (lower) scale vegetation modified GEP and predicted sediment yield. Site location is shown on Figure 1. Initial GEP grid derived from DEM using NetMap.

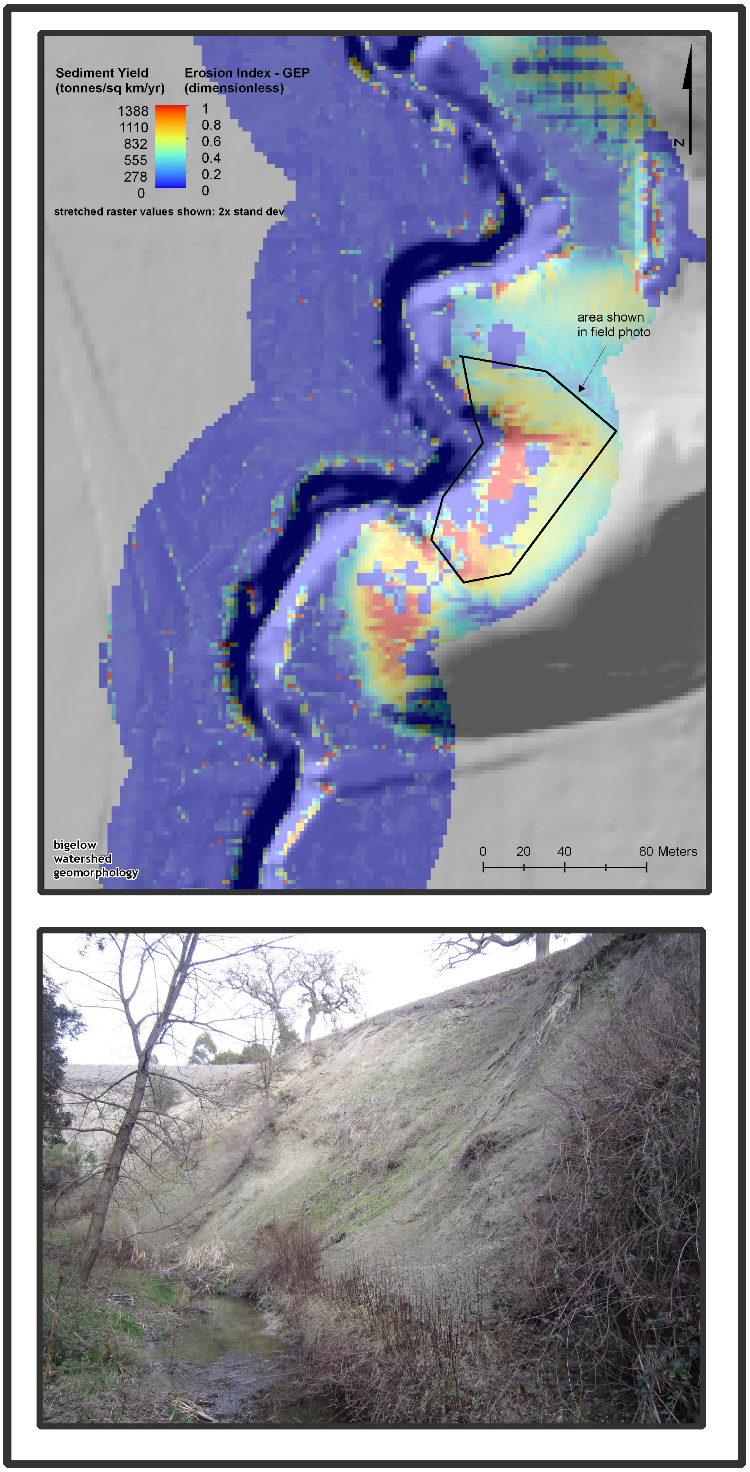

Figure 8. Incised channel eroding into hillslope on Upper Tassajara Creek basin, showing pixel scale vegetation modified GEP and predicted sediment yield draped over 2 m DEM (upper) and field photo of eroding bank. Site location is shown on Figure 1. Initial GEP grid derived from DEM using NetMap

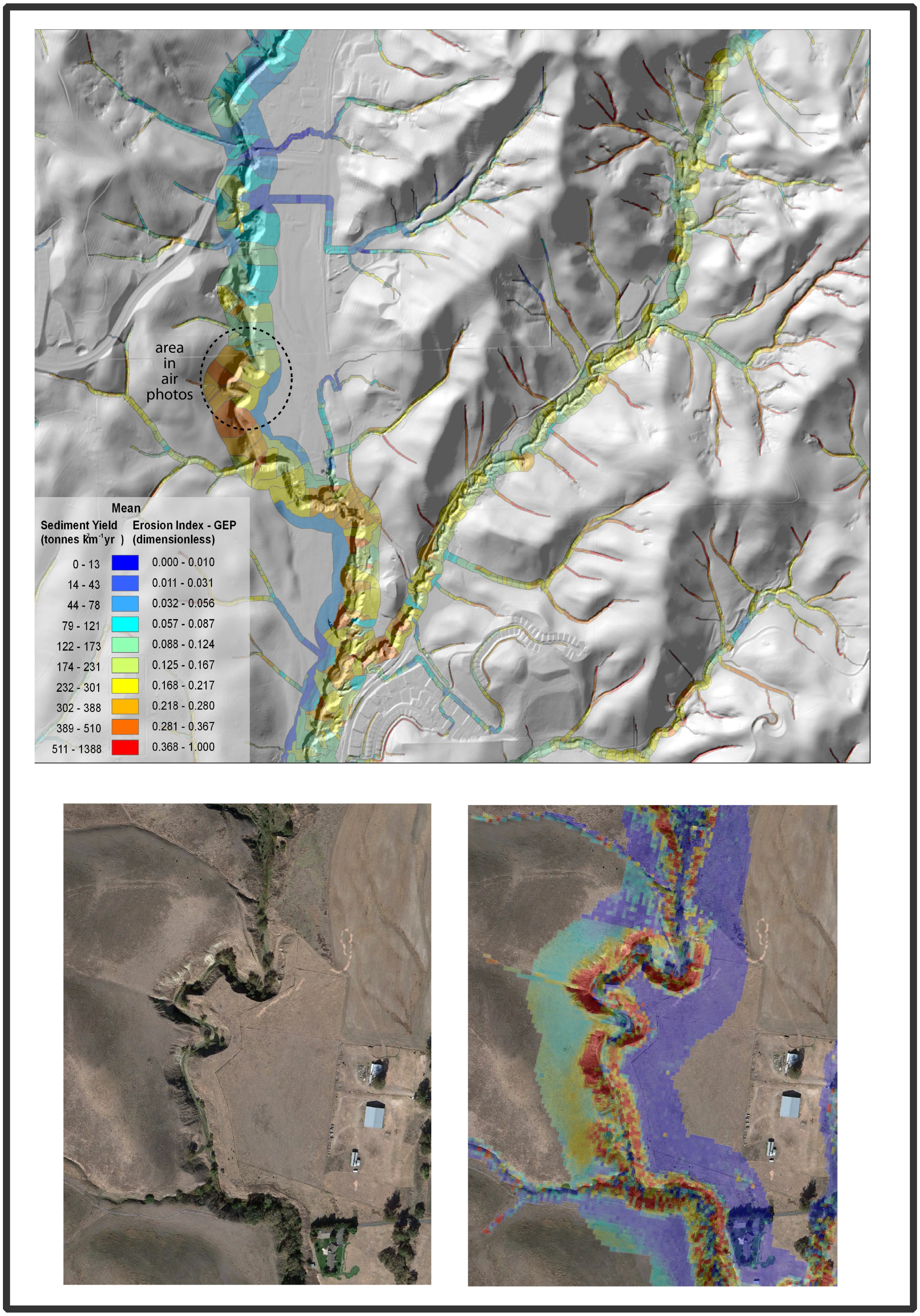

Figure 9. Incised channel on lower Tassajara Creek basin showing vegetation modified GEP and predicted sediment yield at the reach scale (upper) and Google Earth image (lower left) with pixel scale modified GEP draped over image. Site location is shown on Figure 1. Initial GEP grid derived from DEM using NetMap.

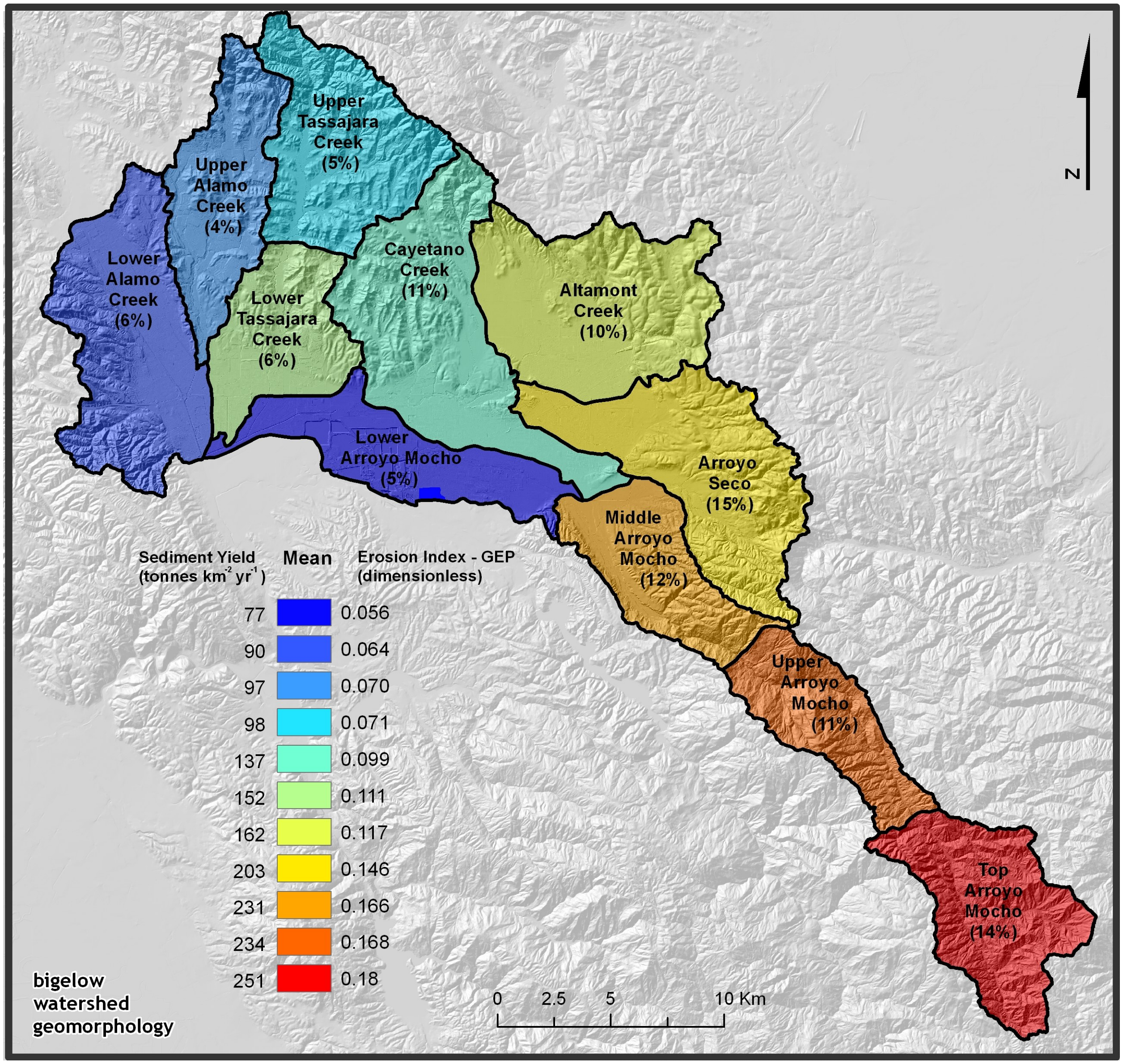

Figure 10. _Average (per unit area)_ vegetation modified GEP and predicted sediment yields for the 11 major basins (HUC 12) in the Arroyo Mocho watershed. Yellow to red areas have estimated erosion rates roughly 200 – 300% greater than blue areas. Values in parentheses are the percentage of the _total_ (i.e. basin as a whole, _not_ per unit area) Arroyo Mocho watershed modified GEP or sediment yield for each basin. Initial GEP grid derived from DEM using NetMap.

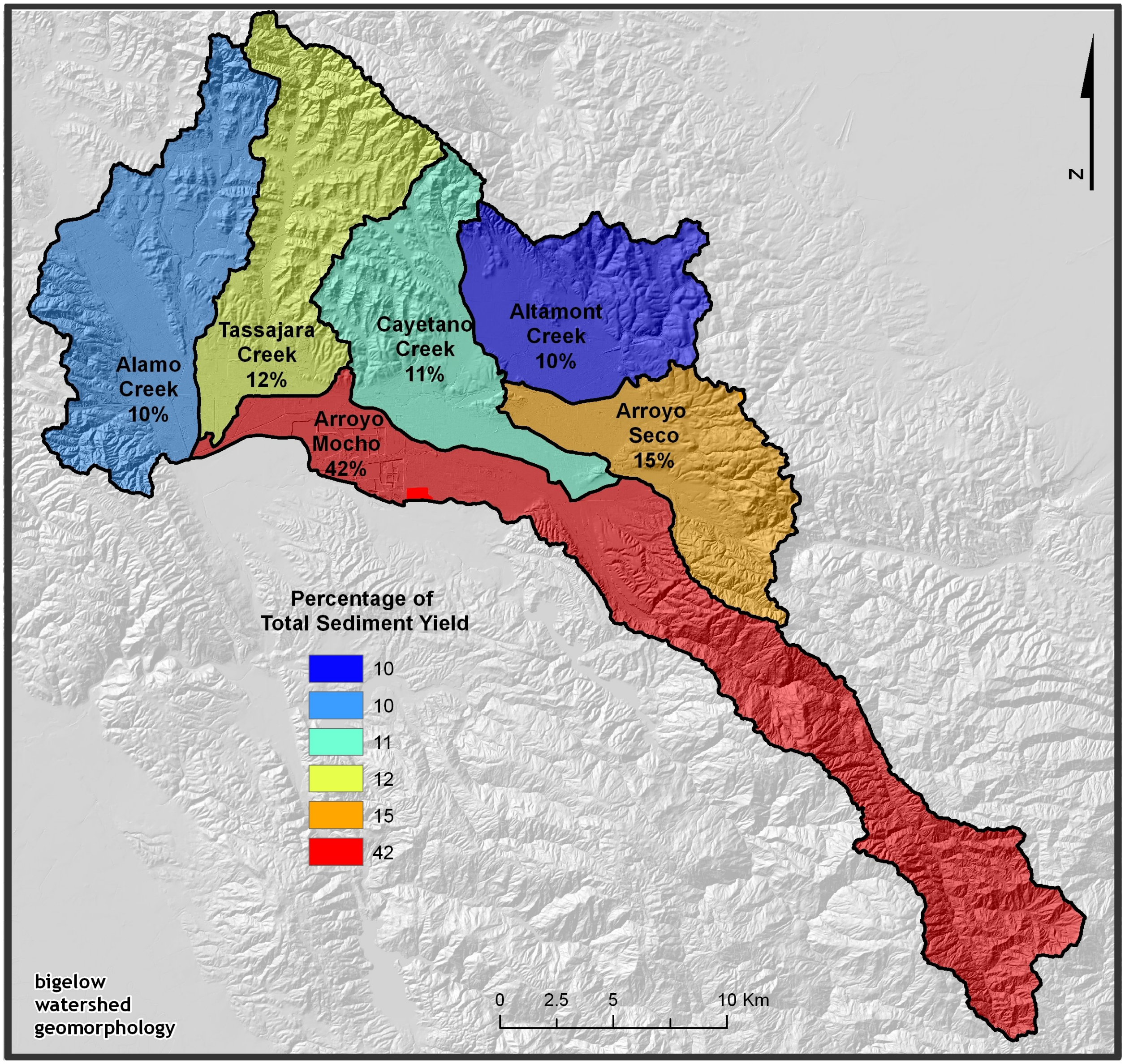

Figure 11. Percentage of the *total* predicted sediment yield for each of the six major tributary basins (i.e total yield for that tributary basin as a whole, *not* per unit area).

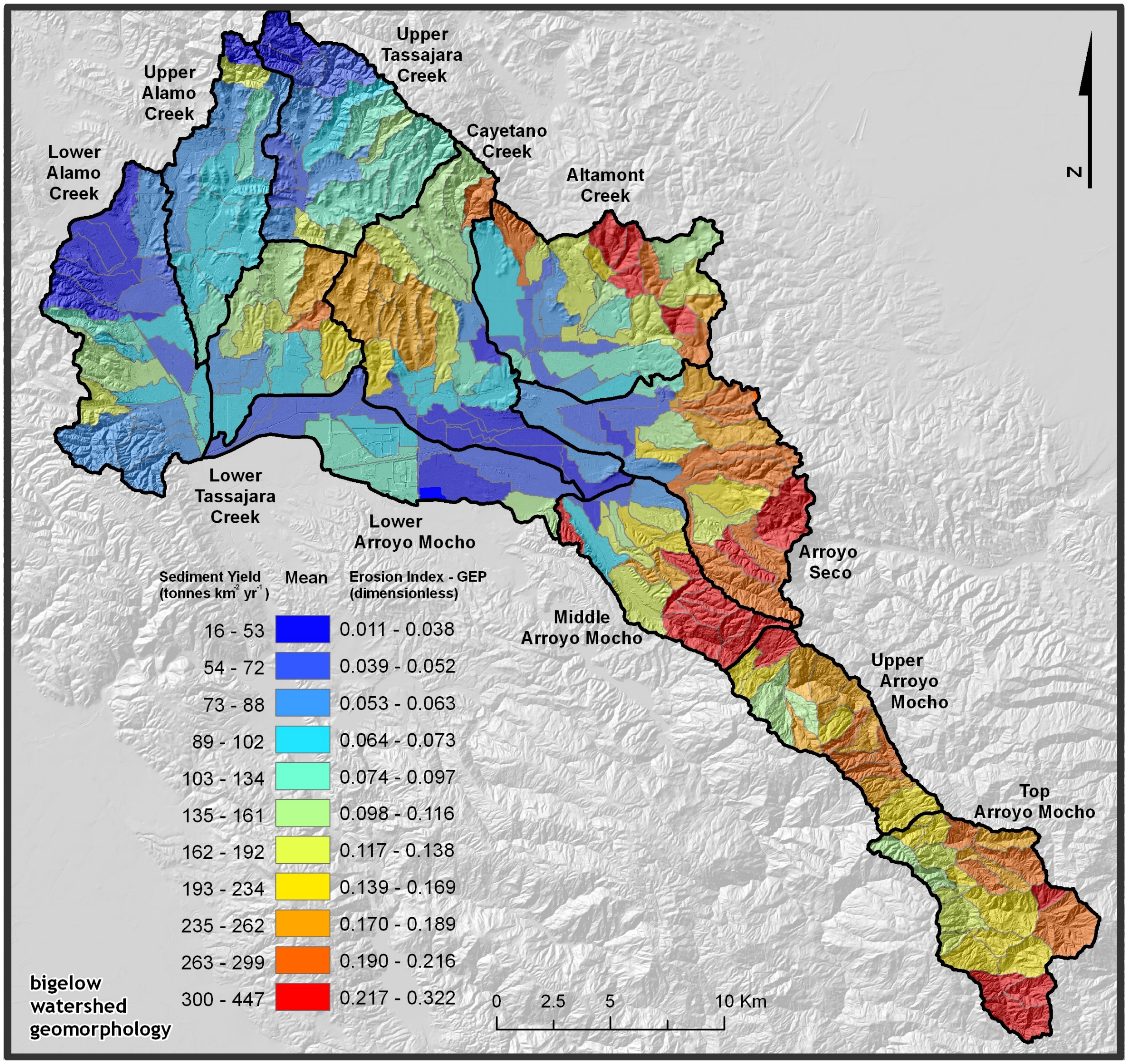

Figure 12. <u>*Average*</u> vegetation modified GEP and predicted sediment yields (<u>*per unit area*</u>) summarized at the subwatershed scale. At this subwatershed scale, yellow to red areas have estimated erosion rates roughly 300 – 800% greater than blue areas. Initial GEP grid derived from DEM using NetMap (Benda et al. 2007, 2011).

or in canyon areas where eroding terraces (Figure 4) or where deep-seated landslides or earthflows impinge on the channel (Figure 5). At the subwatershed scale, yellow to red areas have predicted erosion rates roughly 300 – 800% greater than blue areas (Figure 12). The information displayed in Figure 12 may be useful for prioritizing potential source control activities.

At the subwatershed scale spatial variability in predicted erosion and sediment supply potential can be evaluated at the stream reach scale that often highlights incised areas with banks eroding into steep hillslopes (Figures 7 and 9). At the reach scale, the spatial distribution of erosion can be viewed at the level of individual pixels to identify eroding banks (bare of vegetation) (Figures 4 - 9). The spatial distribution of GEP and predicted sediment yield at these four scales provides a physical basis for evaluating and prioritizing sediment sources within the large 573 km^2 Arroyo Mocho watershed.

Sediment Aggregation Downstream and Sediment Storage. NetMap was used to aggegate (summed and area weighted) the predicted sediment yields through the stream network at the scale of stream segments to illustrate how sediment yield varies downstream through the channel network (Figure 13). The information displayed in Figure 13 is also useful for prioritizing potential source control activities at a finer scale, showing which channels to focus on, rather than entire subwatersheds (Figure 12). Similar to the previous terrain mapping summaries (Figures 10 - 12), this channel reach scale analysis illustrates higher sediment supply from the more dissected steep terrain of Arroyo Mocho canyon. We also aggregated the total sediment yield downstream by segment and divided it by the total load to show the percentage of the load by tributary (Figure 14). The estimation of sediment supply to channels represents a preliminary partial sediment budget (e.g. Reid and Dunne 1996), based on predictions as described above and on limited field observations that steeper and more convergent terrain have a higher erosion (primarily bank erosion and gullying, but also shallow landsliding and surface erosion) and thus a higher sediment supply to channels.

Using equation (6), sediment storage potential is predicted to vary considerably across the stream network. Certain portions of the mainstems are predicted to have a higher potential sediment storage compared to other segments (Figure 15). The higher sediment storage potential reflects a combination of terrain attributes that would encourage sediment deposition (wide valleys and low channel gradients, see methods). These predictions do not capture areas prone to sediment storage from channel constrictions (e.g. bridges, Lung 2010) or confluence effects that may exert primary control on aggradation in Zone 7 flood control channels.

Limitations and Recommendations

Here we provide some initial recommendations for characterizing and mitigating sediment sources based on this study. The recommendations for additional characterization describe some of the limitations of our terrain mapping study and potential improvements. The recommendations are listed in order of decreasing importance and priority.

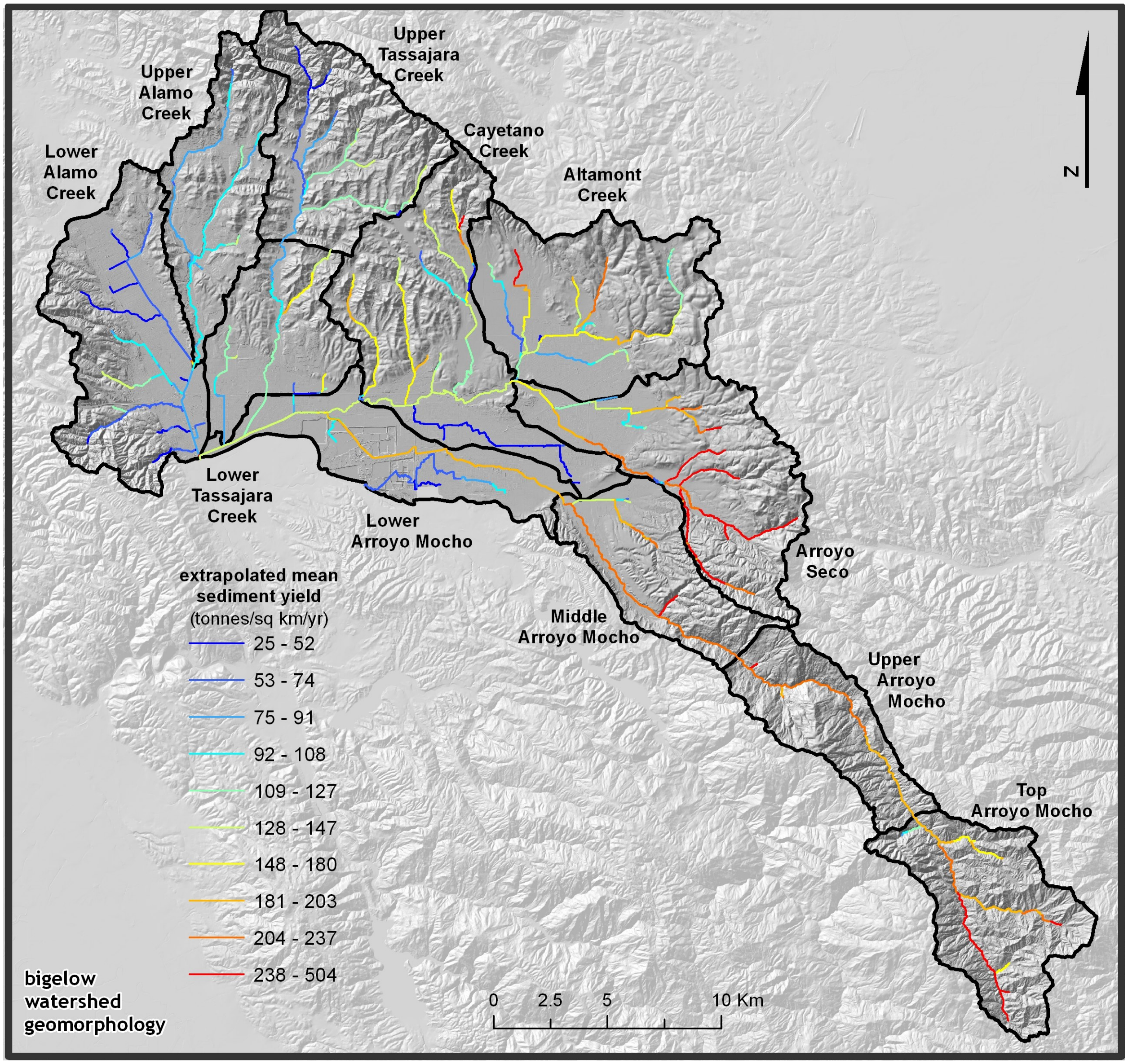

Figure 13. Predicted sediment yield (per unit area) aggregated downstream (summed and area weighted) through the stream network for mainstem streams (draining areas > 2 km^2).

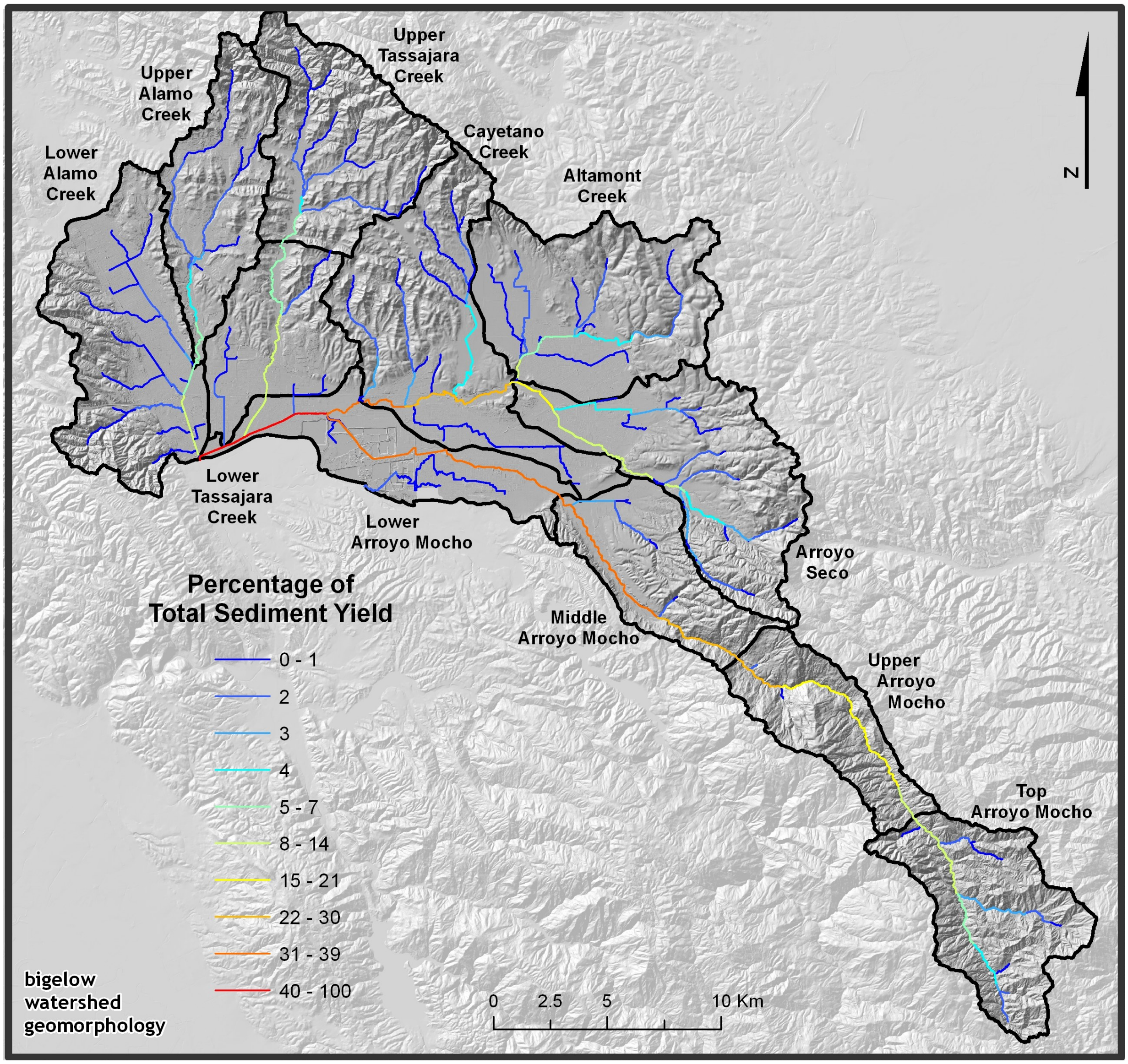

Figure 14. Percentage of *total* predicted sediment yield aggregated downstream through the stream network for mainstem streams (draining areas > 2 km^2).

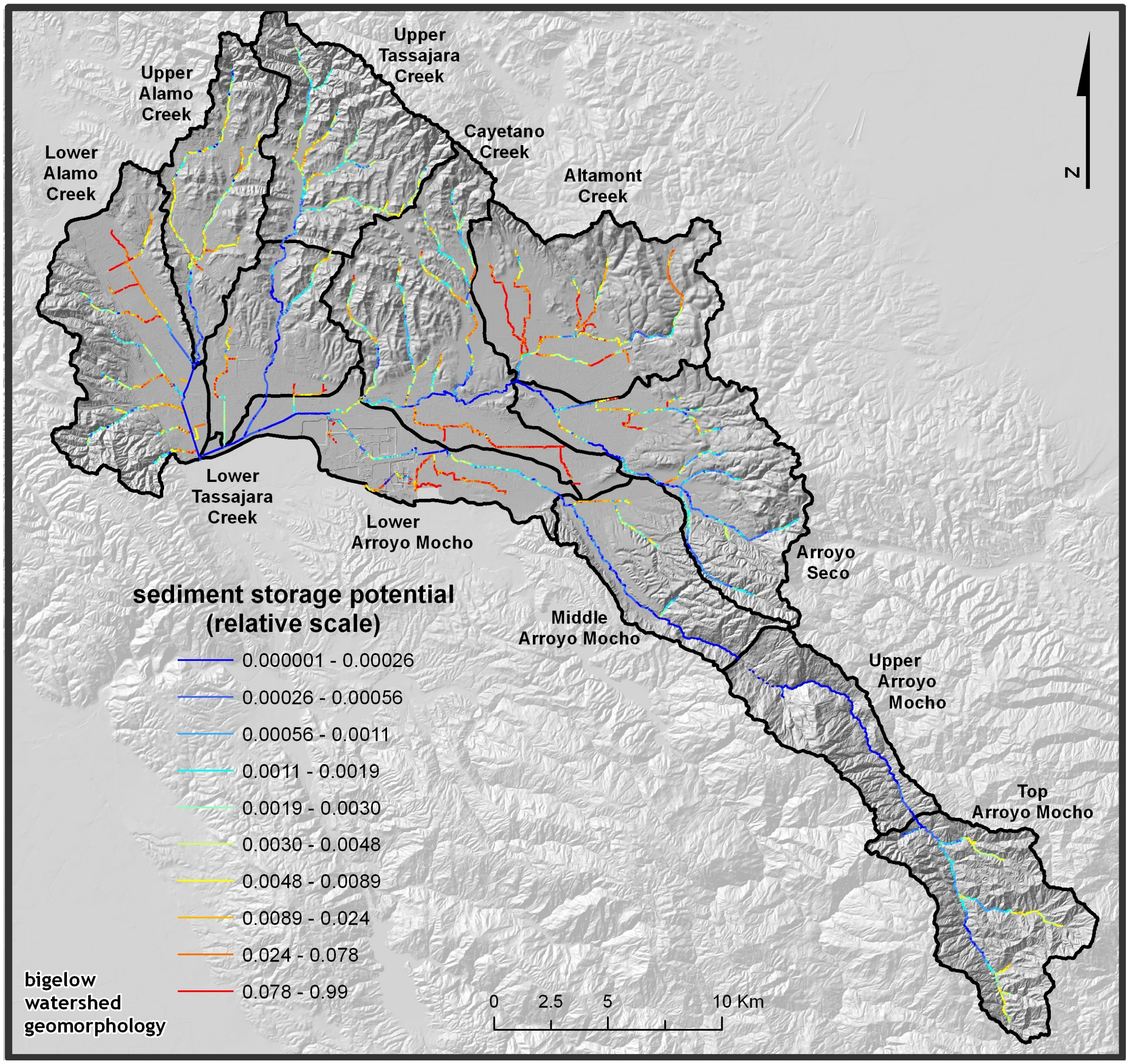

Figure 15. Predicted sediment storage potential for mainstem channels (draining areas > 2 km^2) based on valley width index (valley width/channel width) and stream power (drainage area * gradient). Areas with a high valley width index and low stream power are shown in red. These predictions do not capture areas prone to sediment storage from channel constrictions (e.g. bridges) or confluence effects. Valley width, stream gradient, and drainage area parameters derived from DEM using NetMap (Benda et al. 2007, 2011), channel widths predicted from drainage area based on regional regression relationship (Dunne and Leopold 1978).

1) Causes of Incision. The channels of the Arroyo Mocho watershed often have an incised arroyo form with steep and eroding banks. The channels appear to have undergone several phases of incision, and may have historically had an incised arroyo channel form. Clarifying the causes and episodes of incision would help inform mitigation efforts by focusing on the causal mechanism (e.g. valley floor channelization, altered riparian vegetation, increased suburban runoff, etc., also see Rogers 1988). This would require a combination of literature and air photo review and some field work.

2) Sediment Source Control. Based on our brief field observations, we describe two potential strategies that might be considered in sediment management plans for Zone 7 flood control channels:

a) Promote Riparian Vegetation Growth. The link between channel stability and riparian vegetation is well established (e.g. Thorne 1990, Simon and Darby 1999, Abernethy and Rutherford 2001). Using comparative cross sections from 1957 and 1988, Rogers (1987) indicates substantial incision and loss of riparian trees in several Contra Costa County channels, including Alamo Creek in Zone 7. To encourage riparian growth in bare and eroding areas, strategies could be employed including tree and shrub planting and exclusion of cattle from riparian areas. Bare but not actively eroding areas and incised areas that are trending towards stabilization (i.e. starting to form an inner floodplain) are probably best candidates for riparian restoration (Fischenich and Morrow 2000). Such areas could be prioritized based on the characterization of sediment supply in this report and further study described in this section. This approach requires the cooperation of land owners and could be eligible for funding from Federal and State grants.

b) Promote Sediment Sinks and Floodplain Deposition on Valley Floors. Historically the Livermore Valley floor was a sediment sink, where tributaries deposited sediment as broad coalescing fans across the valley floor and a constriction of the valley at the outlet to Arroyo de la Laguna created a depositional lagoon (Figure 1). While opportunities to reconnect channels to Livermore Valley floor floodplains may be limited by suburban development near channels, there may be more opportunities to promote sediment storage on tributary valley floors. Indeed this appears to be a strategy downstream of suburban development in some basins, such as Upper Alamo Creek, and smaller scale cattle ponds that trap sediment from highly disturbed areas (Figure 16A). We also observed some basins where the channel disappears into flat valley bottoms that store sediment. There may be some locations on the Livermore Valley floor that could be targeted for sediment storage, where there is sufficient space to allow channels to reoccupy floodplains or become multithread channels (Figure 16B). Ideal locations for promoting sediment storage could be identified based on valley width, stream gradient, and other attributes contained in the NetMap stream layer and prioritized based on the characterization of sediment supply (e.g Figures 12 and 13) in this report, the forthcoming historical ecology analysis for Zone 7, and further characterization described in this section.

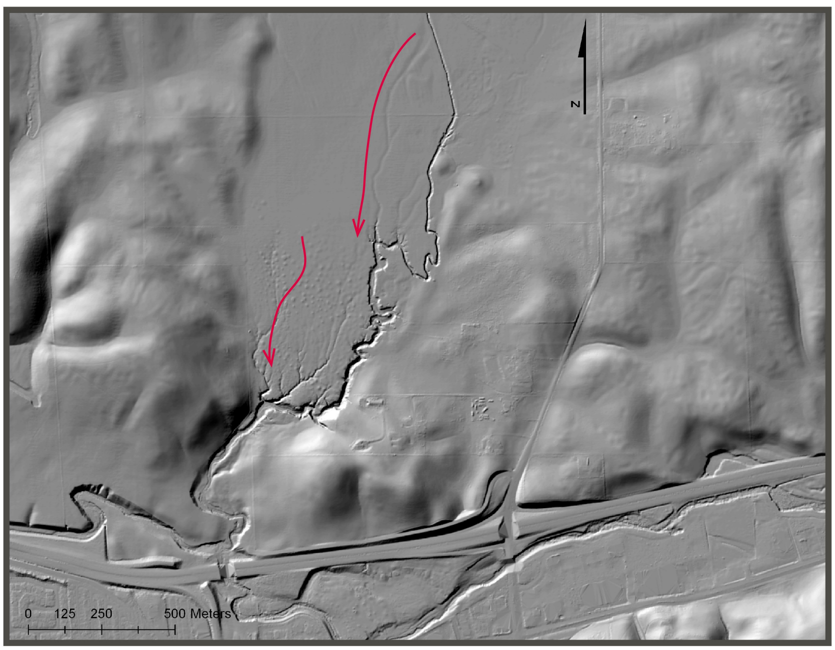

Figure 16. (16A upper) Example of a stock pond in upper Tassajara Creek that traps sediment below a highly disturbed valley floor. (16B lower) Example of an area that could promote sediment storage in lower Cayetano Creek, where a “plug and pond” style restoration project could recreate a multithread channel connected to its floodplain. The US Forest Service commonly restores incised meadow areas using such an approach where the incised channel is plugged with check dams or filled and new channels are reconnected to the floodplain.

3) Sediment Supply from Earthflow Terrain. GEP generally captures erosion sources driven by steep and convergent slopes, but does not adequately capture lower gradient sediment sources such as earthflows. GEP may be an adequate indictor of the erosion potential at earthflow toes, however, it does not address the rate of erosion. Earthflows tend to move after cumulative weeks and months of heavy precipitation (Keefer and Johnson 1983, Rogers 1987). Short term rates of earthflow movement in the Eastbay hills range from centimeters per year in the Berkeley hills over 9 years (Hilley et al. 2004) to meters per year in the Castro Valley hills over one year (Keefer and Johnson 1983). Earthflows can dominate sediment supply to channels in the Coast Range (e.g. Kelsey 1977, Bedrossian and Custis 2002, Mackey and Roering 2011). Hummocky terrain characteristic of earthflows is apparent on high resolution hillshade maps, particularly in the northern tributary basins with clay rich formations (e.g. Figure 18 upper, also see Davenport 1985, Wentworth et al. 1997, Roberts et al. 1999, Majmundar 1991 and 1996). Characterizing sediment supply from earthflows would entail compiling past mapping of earthflows, improved mapping from high resolution LiDAR hillshade maps, and some characterization of earthflow activity and rates from the field and literature.

4) Episodic Sediment Supply. The predicted sediment supply in the terrain analysis represents an average condition using only topographic attributes that characterize *chronic or annual (persistent)* sediment supply (primarily bare steep channels banks). However, erosion and sediment supply from most landscapes are highly variable in space and time resulting from highly stochastic processes driven by interactions among storms, vegetation and topography (Benda and Dunne 1997). The terrain mapping approach generally characterizes sediment supply from bank erosion and small streamside slides that appear to dominate. However, episodic mass wasting from hillslope areas further from the steams may be triggered during more extreme events such as El Niño storms (e.g. Ellen and Wieczorek 1982). Such events can dominate the long term sediment supply on the Alameda Creek system, for example, El Niño events in 1983 and 1998 (Figure 2) accounted for 37% of the total load at Niles gage (1970-2010) (Beagle et al. 2012) and a 1958 flood event comprised 48% of the total load at Niles (1957-1970) (Brown and Jackson 1973). Patchy remnant fill terraces created by the 1950s extreme floods are occasionally visible in the higher order channels of the Alameda Creek watershed today (Bigelow et al. 2008, Pearce et al. 2009, Beagle et al. 2012) and we observed such fill terraces in the Arroyo Mocho canyon (Figure 17).

Some characterization and comparison of the episodic and chronic (persistent) sediment supply could be used to deterimine: (1) what proportion of the long-term sediment supply is dominated by episodic events and (2) the spatial distribution of sediment sources from episodic supply. Characterizing the episodic supply of sediment from past hillslope mass wasting would entail generating a landslide inventory from historic air photos spanning large storm events and some field work to estimate the input from shallow streamside slides not easily visible on air photos and sampling of large landslide scarp depths that cannot be estimated from air photos.

These hillslope mass wasting sources are generally natural (Figure 18) and mitigation opportunities may be limited to opportunistic and untested vegetation restoration of native bunch grasses. Kelsey (1977, 1978) suggested the conversion of deep-rooted native bunch

Figure 17. Cut and fill terraces (~2m high) observed in Arroyo Mocho canyon just downstream of massive earthflow sources. Sycamores on the floodplain/terrace tread in the lower photo appear to be greater than 50 years old, possibly dating to the historic 1950s floods.

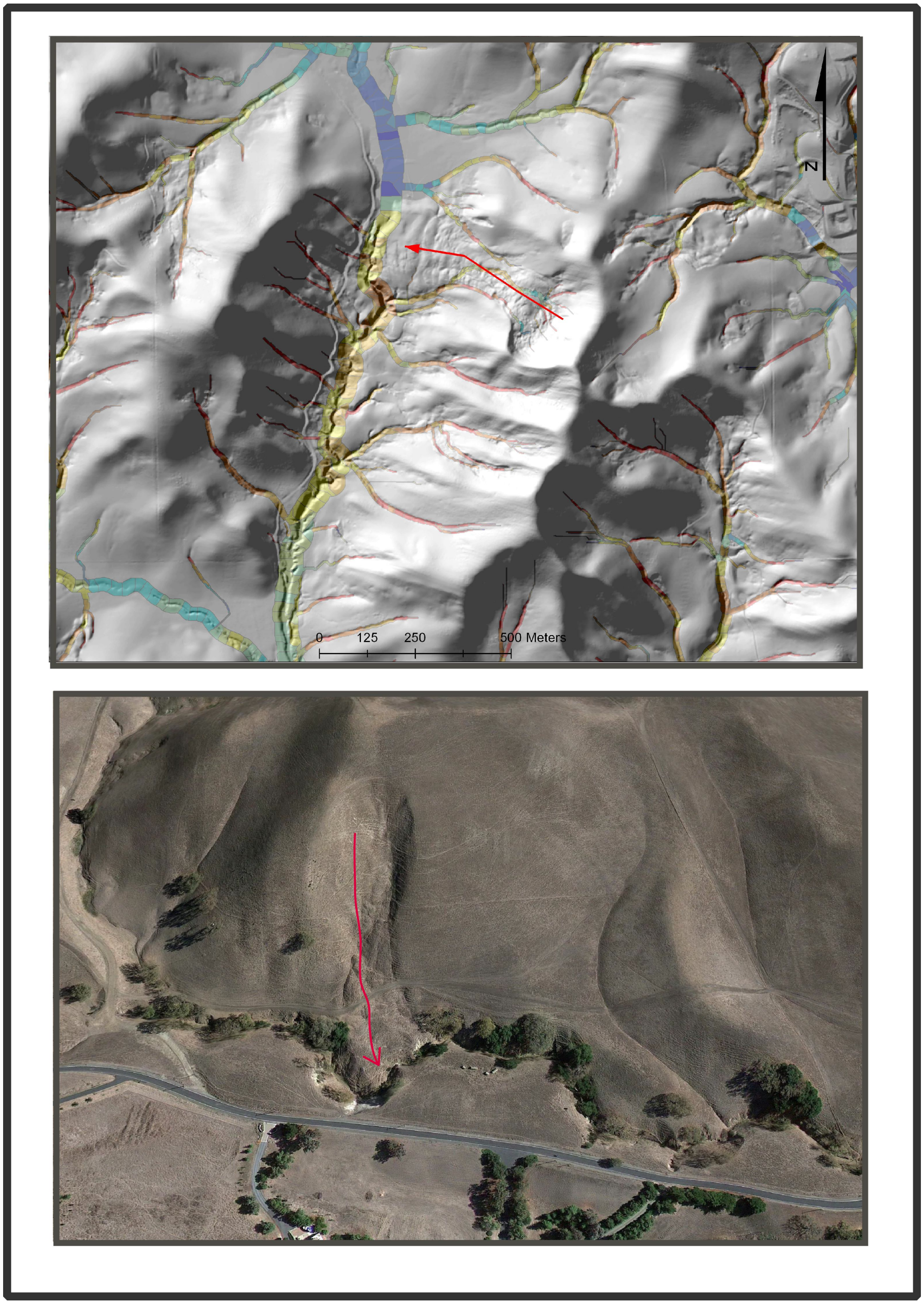

Figure 18. Examples of mass wasting in Cayetano Creek basin that are likely triggered and move episodically during large storms or months of heavy precipitation. Sediment supply from such episodic supply is not fully captured by the terrain mapping estimates of chronic sediment supply characterized in this study. The GEP index captures the steep and convergent landform of the earthflow toe, however, it does not address erosion rates which might be accelerated compared to other, non earthflow related, arroyo landforms.

grasses to shallow-rooted annual grasses for cattle grazing by early settlers may have caused a substantial increase in the sediment flux to channels from earthflows on the Van Duzen River in Northern California, and other historical grazing impacts on sediment supply have been hypothesized for the East Bay hills (Reid 1987). A more detailed analysis and literature review of mitigation opportunities from mass wasting could also be conducted.

5) Improved Mapping of Incised Channels. Channel incision and gullying in the Arroyo Mocho watershed is discontinuous or patchy. In this study we used digital terrain modeling (NetMap using GEP) to characterize erosion from steep banks of incised channels. However, it may be possible to improve the identification and mapping of incised channels. This would entail developing a new analysis tool in NetMap that would define the width and depth of channel incision throughout the channel network by locating the break in slope between the natural hillslope or valley floor and the steep incised channel bank.

6) Sediment Caliber. This terrain mapping approach characterizes total sediment supply to the stream network without regard to sediment caliber. Some characterization of sediment caliber supplied and transported through the stream network would help prioritize potential mitigation efforts to sources that have a higher bedload component filling the valley floor flood control channels. For example, harder Franciscan rocks underlying the upper Arrroyo Mocho watershed may result in a larger bedload component compared to the northern tributaries underlain by weaker lithologies. This type of characterization could involve tumbling mill analysis of colluvium throughout the watershed to estimate attrition rates combined with sediment transport estimates/modeling (e.g. Collins and Dunne 1989, Benda and Dunne 1997). Additionally, the ratio of bedload to total load is known to vary with drainage area (higher bedload ratios in smaller basins) and a relationship could be developed and applied (along with predictions of bedload attrition) to make predictions of grain size in concert with predictions of sediment supply along the channel network.

References

Abernethy B, Rutherford ID. 2001. The distribution and strength of riparian tree roots in relation to riverbank reinforcement. Hydrological Processes 15: 63–79.

Beagle, J.R., Bigelow, P., McKee, L. J., Pearce, S. 2012. Sediment Source Reconnaissance of Stonybrook and Sinbad Creek Watersheds: A rapid evaluation of two small tributaries near the Alameda Creek Flood Control Channel. Prepared for the Alameda County Flood Control and Water Conservation District.

Bedrossian, T.L. and K. Custis. 2002. Review of July 2002 EPA Analysis of Impacts of Timberland Management on Water Quality. California Geologcial Survey Memorandum. ftp://ftp.consrv.ca.gov/pub/dmg/thp/documents/memorandas/EPA.pdf

Beeson, C.E, and Doyle. P .E, 1995, Comparison of bank erosion at vegetated and non-vegetated channel bends. Water Resources Bulletin, vol. 31, no. 6, p. 983-990.

Benavides-Solorio, J. and L. H. MacDonald, 2005. Measurement and prediction of post-fire erosion at the hillslope scale, Colorado Front Range. International Journal of Wildland Fire 14:1-18.

Benda, L. and Dunne, T. 1997. Stochastic forcing of sediment routing and storage in channel networks. Water Resources Research, v.33: 2865-2880.

Benda, L., Miller, D. J., Andras, K., Bigelow, P., Reeves, G., and Michael, D. 2007. NetMap: A new tool in support of watershed science and resource management, Forest Sci., 52, 206–219.

Benda, L., Miller, D., Lanigan, S., and Reeves, G. 2009. Future of applied watershed science at regional scales, EOS, T. Am. Geophys. Un., 90, 156–157.

Benda, L., Miller, D., and Barquín, J. 2011. Creating a catchment perspective for river restoration, Hydrol. Earth Syst. Sci. Discuss., 8, 2929-2973, doi:10.5194/hessd-8-2929-2011.

Bigelow, P., S. Pearce, L. McKee, and A. Gilbreath. 2008. A sediment budget for two reaches of Alameda Creek. Prepared for Alameda Flood Control and Water Conservation District.

Brown, W.M. and L.E. Jackson. 1973. Erosional and depositional provinces and sediment-transport in the south central San Francisco Bay region, California: San Francisco Bay Environment and Resources Planning Study, Interpretative Report 3, U.S. Department of the Interior, Geological Survey Miscellaneous Field Studies Map 515, U.S. Department of Housing and Urban Development, 3 sheets.

Clarke, S., Burnett, K. M., and Miller, D. J. 2008. Modeling streams and hydrogeomorphic attributes in Oregon from digital and field data, J. Am. Water Resour. Assoc., 44, 459–477.

Collins, B., and T. Dunne. 1989. Gravel transport, gravel harvesting and channel-bed degradation in rivers draining the southern Olympic Mountains, Washington, U.S.A., Environ. Geol. 13:213-224.

Davenport, C.W. 1985. Landslide Hazards in Parts of the Diablo and Dublin 7.5' Quadrangles, Contra Costa County, California. California Division of Mines and Geology Open-File Report 86- 7 SF, Landslide Hazard Identification Map No. 3.

Dietrich, W.E. and T. Dunne, 1978. Sediment Budget for a Small Catchment in Mountainous Terrain: Zietschrift fur Geomorphologie, Suppl. 29:191-206.

Dunne, T., and L.B. Leopold. 1978. Water in environmental planning. W. H. Freeman & Company. San Francisco. 818 p.

Emmett, W.H. 2004. A historical perspective on regional channel geometry curves. Stream Notes - January. U.S. Forest Service Streams Systems Technology Center.

Ellen, S. and Wieczorek, G.F., editors. 1988. Landslides, floods, and marine effects of the storm of January 3-5, 1982, in the San Francisco Bay region, California: U. S. Geological Survey Professional Paper 1434

Fischenich, J.C., and Morrow, J.V. 2000. Reconnection of floodplains with incised channels. US Army Engineer Research and Development Center Technical Notes Collection (ERDC-TN-EMRRP-SR-09).

Gilman, E. 1988. Predicting root spread from trunk diameter and branch spread. Journal of Arboriculture 14(4): 85–89.

Grant, G.E., Swanson, F.J. 1995. Morphology and processes of valley floors in mountain streams, western Cascades, Oregon. Natural and Anthropogenic Influences in Fluvial Geomorphology. Geophysical Monograph, vol. 89, pp. 83–101.

Graymer, R.W., Jones, D.L., and E.E. Brabb. 1996. Preliminary geologic map emphasizing bedrock formations in Alameda County, California: A digital database. USGS Open-File Report: 96-252.

Helley, E.J., and Graymer, R.W. 1997. Quaternary geology of Alameda County, and parts of Contra Costa, Santa Clara, San Mateo, San Francisco, Stanislaus, and San Joaquin Counties, California: A digital database. USGS Open-File Report: 97-97.

Hilley GE, Burgmann R, Ferretti A, Novali F, Rocca F. 2004. Dynamics of slow-moving landslides from permanent scatterer analysis. Science 304(5679): 1952–1955.

Keefer, D.K., and Johnson, A.M., 1983. Earth flows – Morphology, mobilization and movement. U.S. Geological Survey Professional Paper 1264.

Kelsey, H. M. 1977. Landsliding, Channel Changes, Sediment Yield and Land Use in the Van Duzen River Basin, North Coastal, California: Ph.D. Dissertation, Published in Earth Resources Monograph 3, U. S. Forest Service Region 5, 370 p.

Kelsey, H. M. 1978. Earthflows in Franciscan Melange, Van Duzen River Basin, California: Geology, v. 6, p. 361-364

Lung, P., 2010. Sediment and hydraulic challenges in the city of Livermore. Alameda Creek Watershed Council Annual Conference. October 28. Castro Valley, CA.

Mackey, B.H. and J.J. Roering. 2011. Sediment yield, spatial characteristics, and the long-term evolution of active earthflows determined from airborne LiDAR and historical aerial photographs, Eel River, California. Geol Soc Am Bull 123:1560–1576.

Majmundar, H.H., 1991. Landslide Hazards in the Livermore Valley and Vicinity, Alameda and Contra Costa Counties, California, Calif. Div. Mines and Geology Open-file Report 91-02, Landslide Hazard Identification Map 21. Map scale 1:24,000.

Majmundar, H.H., 1996. Landslides and related features, in Landslide hazards in the Hayward quadrangle and parts of the Dublin quadrangle, Alameda and Contra Costa Counties, California: Calif. Div. Mines and Geology, Open-file Report 95-14, plate B, map scale 1:24,000.

Miller, D. J. 2003. Programs for DEM Analysis. Seattle, WA, Earth Systems Institute: 38.

Miller, D. J. and Burnett, K. M. 2007a. Effects of forest cover, topography, and sampling extent on the measured density of shallow, translational landslides, Water Resour. Res., 43, 1–23.

Reid, L.M. and Dunne, T. 1996. Rapid evaluation of Sediment Budgets. Germany: GeoEcology paperbacks, Catena Verlag.

Reid, L.M. 1987. Erosion and deposition in a discontinuous gully system. Ph.D. dissertation, University of Washington, Geological Sciences. 270 pp.

Pearce, S., Bigelow, P., and McKee, L. 2009. Dry Creek Watershed Sediment Source Reconnaissance Technical Memorandum. Prepared for the Alameda County Flood Control and Water Conservation District, Hayward, CA. Regional Watershed Program, San Francisco Estuary Institute, Oakland, CA. 27 pp.

Prism 2012. Oregon State University parameter-elevation regressions on independent slopes model (Prism) climate mapping system and climate data archive: http://www.prism.oregonstate.edu

Rogers, J.D. 1987. Pleistocene to Holocene transition in central Contra Costa County. In n Field Trip Guide to the Geology of the San Ramon Valley and Environs, pp. 29-51. Northern California Geological Society, San Ramon, California.

Roberts, S., M.A. Roberts, and E.M. Brennan. 1999. Landslides in Alameda County, California, A Digital Database Extracted from Preliminary Photointerpretation Maps of Surficial Deposits by T.H. Nilsen in USGS Open-File Report 75-277.

Sidle, R.C. 1987. A dynamic model of slope stability in zero-order basins. International Association of Hydrological Sciences, Publication 165:101-110.

Simon A, Darby SE. 1999. The nature and significance of incised river channels. In Incised River Channels: Processes, Forms, Engineering and Management, Darby SE, Simon A (eds). John Wiley and Sons: London; 3–18.

SFEI. 2011. Bay Area Aquatic Resource Inventory Basemap. San Francisco Estuary Institute, Richmond, CA. http://www.sfei.org/BAARI

Smith, J.G. 1964. Root spread can be estimated from crown width of Douglas Fir, Lodgepole Pine, and other British Columbia tree species. The Forestry Chronicle 40(4): 456-473.

Strahler, A.N. 1957. Quantitative analysis of watershed geomorphology. Tran. Am. Geophys. Union 38:913–920.

Thorne CR. 1990. Effects of vegetation on riverbank erosion and stability, In Vegetation and Erosion: Processes and Environments, Thornes JB (ed.). John Wiley & Sons: 125–144.

Tubbs, C.H. 1977. Root-crown relations of young sugar maple and yellow birch. Research Note NC-225. USDA Forest Service, North Central Forest Experiment Station.

Wang, Z.Y., G.H. Huang, G.Q. Wang, and J. Gao. "Modeling of Vegetation-Erosion Dynamics in Watershed Systems." Journal of Environmental Engineering. Vol 130, No. 7, July 1, 2004.

Wentworth Carl M., Scott E. Graham, Richard J. Pike, Gregg S. Beukelman, David W Ramsey, Andrew D. Barron. 1997. Summary Distribution of Slides and Earth Flows in Alameda County, CA. USGS OF 97-745.